Proceedings of Combustion Institute – Canadian Section
Spring Technical Meeting
University of Manitoba, Winnipeg
May 8-11, 2011

Ignition timing criteria for partial burn operation in an HCCI engine

Ahmad Ghazimirsaied[1], Mahdi Shahbakhti[2], Charles Robert Koch[1]*

[1]*Department of Mechanical Engineering, University of Alberta, Edmonton, Canada*
[2]*Department of Mechanical Engineering, University of California, Berkeley, USA*

1. Abstract

Homogeneous Charge Compression Ignition (HCCI) has the potential to improve the efficiency of Spark Ignition (SI) or Compression Ignition (CI) engines particularly at part load near the partial burn/misfire limit. Two challenges of HCCI combustion are: maintaining constant ignition timing despite no direct mechanism to initiate combustion, and to expand the part load region of HCCI near the misfire limit. An accurate criteria of ignition timing is critical to accomplish this.

The crank angle where the maximum pressure occurs (θ_{Pmax}) is proposed as a robust criteria for distinguishing between normal and misfire HCCI combustion modes. Particularly near the partial burn/misfire limit, this method is found to be more reliable than the existing methods of $CA50$ (Crank angle of 50 percent mass fraction burned). Using (θ_{Pmax}), normal and partial burn engine cycles can be determined cycle by cycle for fuels exhibiting a cool flame. The performance of this new criteria is then analyzed for different engine loads at both constant fueling and constant equivalence ratio at 329 HCCI experimental operating points, each with 100 cycles of cylinder pressure data. For operating points with high cyclic variation θ_{Pmax} is found to be more reliable than $CA50$. Thus θ_{Pmax} could be used in future feedback algorithms to help control to stabilize ignition timing in these regions extending the useful operating range of HCCI.

2. Introduction

HCCI combustion has potential for improved fuel economy, very low oxides of nitrogen (NOx) and low particulate emissions. HCCI is considered as a high-efficiency alternative to spark-ignited (SI) gasoline operation and as a low-emissions alternative to traditional diesel compression ignition (CI) combustion. However, the practical application of HCCI requires overcoming several technical hurdles. HCCI misfire or partial-burn is undesirable because it results in increased exhaust emissions and reduces engine power output. Maintaining proper ignition timing over a wide range of loads and speeds is a challenging problem in HCCI engines [1, 2]. Misfire or partial burn leads to an engine speed decrease [3] and is undesirable since it can lead to speed and torque fluctuations, increased exhaust emissions [4], and unburned fuel in the exhaust that will eventually damage the catalytic converter [5]. In particular, there is a high risk of partial burn or misfire in HCCI operation, which can have a more destructive consequences on engine performance and emissions compared to SI combustion [6, 7].

As fuel flow-rate is decreased, the net heat release rate and average combustion temperature decrease which results in more unburned products-characterized by high CO and unburned HC emissions and by increased cycle-to-cycle variations [6]. As the cylinder charge is made leaner (with excess air) or more dilute (with a higher burned gas fraction from residual gases or exhaust gas recycle) the cycle-by-cycle combustion variations increase until some partial burn cycles occur. Further leaning or more charge dilution results in reaching the misfire limit as a portion of the cycles fail to ignite.

The position of Start of Combustion (SOC) plays an important role in cyclic variations of HCCI combustion with less variation observed when SOC occurs immediately after top dead centre (TDC) [8, 9]. Higher levels of cyclic variations are observed in the main (second) stage of HCCI combustion compared with that of the first stage for the Primary Reference Fuel (PRF) fuels studied. Cyclic variation of SOC is a function of charge properties and increases with an increase in the EGR rate, but decreases with an increase in equivalence ratio, intake temperature, and coolant temperature [10].

The dynamics of HCCI near the partial burn operating region are complex and can require control to avoid misfires [11]. The understanding of the HCCI engine behavior in case of misfire and delayed combustion is an important first step to

*Corresponding author: bob.koch@ualberta.ca

provide a control strategy to avoid partial burn and misfire and expand this HCCI operation region. Some techniques for partial burn recognition use: in-cylinder pressure [12], ionization current [13] and crankshaft angular speed [14]. Here, a method to detect partial burn in terms of a crank-angle based parameters and cylinder pressure are proposed.

In the next section, a single cylinder engine, which is used to collect the data, is briefly described. Then, θ_{Pmax}, a new ignition timing criteria is proposed. The performance of θ_{Pmax} for a specific partial burn operating condition is compared to $CA50$ (common ignition timing method) for this case. Correlations of θ_{Pmax} with maximum cylinder pressure and $CA50$ and the correlations of the cyclic variations are discussed in the next section. Finally, the effect of θ_{Pmax} on $IMEP$ in two different scenarios of constant and varying fueling rate for several operating points is investigated in order to evaluate the θ_{Pmax} criteria as HCCI engine load changes.

3. Engine Setup A single cylinder Ricardo Mark III engine with a Rover K7 head are used to carry out the HCCI experiments [15] and is shown schematically in Figure 1. The engine with specifications given in Table 1 [16] is outfitted with a Kistler in cylinder pressure transducer. Cylinder pressure is recorded 3600 times per crank revolution for 100 cycles, and then analyzed for the pertinent combustion metrics, such as θ_{Pmax}, CA50 and IMEP (Indicated Mean Effective Pressure). All other parameters are logged at 100 Hz. All of the engine operating points are at steady-state operating conditions (inputs to engine and engine speed held constant). Details of 329 engine experimental points from the Ricardo engine are listed in Table 2. The intake air is heated with a temperature controlled 600W electric heater, while the intake pressure is adjusted with an externally driven supercharger. N-heptane and iso-octane are individually port injected to set octane values with two injectors that are individually controlled.

Table 1: Configuration of the Ricardo single-cylinder engine [16]

Parameters	Values
Compression Ratio	10
Bore × stroke [mm]	80 × 88.9
Connecting Rod Length [mm]	159
Displacement [L]	0.447
Valves	4
IVC [aBDC]	55
EVO [aBDC]	-70

Table 2: Engine operating conditions

Parameter	Range
Manifold Temperature [°C]	60-161
Fuel Octane Number [PRF]	0,10,20,40
Manifold Pressure [kPa]	88-162
Equivalence Ratio [-]	0.29-0.95
External EGR [%]	0-30
Engine Speed [RPM]	760-1340
Coolant Temperature [°C]	25-84
Oil Temperature [°C]	48-80

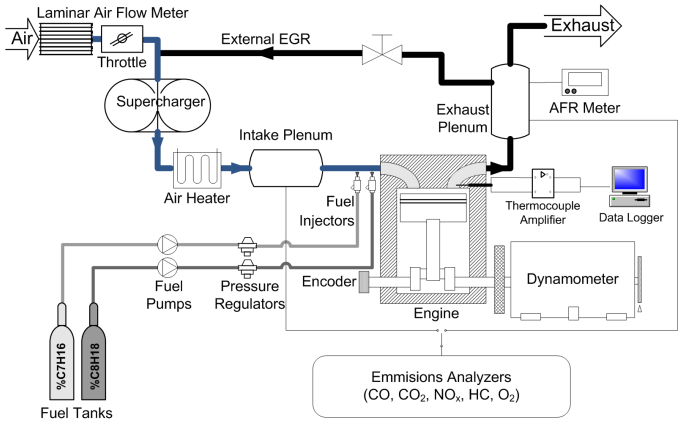

Figure 1: Schematic of the experimental setup [16]

4. Experimental Results and Discussion

Ignition Timing

θ_{Pmax} is defined as the crank angle of the maximum in-cylinder pressure during one engine cycle. θ_{Pmax} is used as ignition timing parameter as it is simple and requires minimum computational resources [17] and using heat release analysis the cyclic variability in ignition timing, θ_{Pmax}, is compared to other common criteria and is found to be robust [7, 18, 19]. θ_{Pmax} also depends predominantly on the phasing of combustion and is independent of charge variations which makes it a useful measure of variability in combustion phasing [18]. With early or late combustion, θ_{Pmax} is a representation of the heat release phasing since it is closely coupled to the combustion volume. An example of the location of θ_{Pmax} for HCCI combustion is shown in Figure 2 where cylinder pressure is plotted versus crankangle. The

location of $CA50$ is also shown in Figure 2 and, in this case, closely matches θ_{Pmax}.

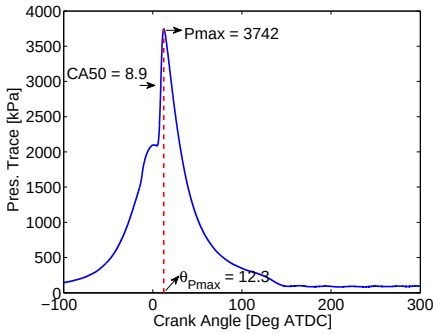

Figure 2: Sample operating point for HCCI combustion at point A. Conditions: PRF 0, engine speed n = 800 rpm, $T_{man} = 120\,^{\circ}$C, $P_{man} = 93$ kPa, $\phi = 0.51$, EGR = 0%, $T_{coolant} = 75\,^{\circ}$C, $T_{oil} = 67\,^{\circ}$C

Comparison of Ignition Timing Criteria

The cyclic variation of ignition timing for two criteria of θ_{Pmax} and $CA50$ are shown in Figure 3 for a portion of consecutive engine combustion cycles for an operating point, denoted A, and shows that the cyclic variation of θ_{Pmax} is higher than $CA50$ indicating higher sensitivity of θ_{Pmax}. In particular θ_{Pmax} captures the one cycle of early ignition timing when misfire occurs at cycle 44 while CA50 does not.

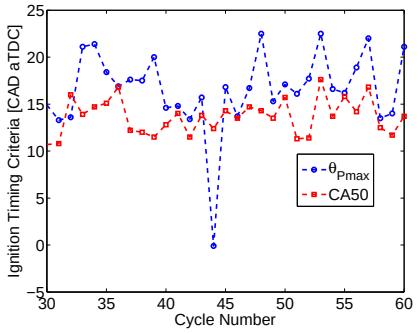

Figure 3: θ_{Pmax} and $CA50$ of consecutive cycles for HCCI combustion for operating point A: PRF 0, n = 1000 rpm, $T_{man} = 100\,^{\circ}$C, $P_{man} = 93$ kPa, $\phi = 0.57$, EGR = 0%, $T_{coolant} = 75\,^{\circ}$C, $T_{oil} = 66.2\,^{\circ}$C

The pressure trace for the consecutive misfire and normal engine cycles for the operating point A is plotted in Figure 4. The left plot has only one stage of combustion representing a misfire cycle with $\theta_{Pmax} = -0.1$ [Deg ATDC] while the second plot shows the next cycle indicating a normal cycle with $\theta_{Pmax} = 16.8$ [Deg ATDC]. The large difference in θ_{Pmax} values for normal and misfire cycles can be used to distinguish between these different combustion modes particularly near the partial burn and misfire region of the engine. Conversely, $CA50$ a very common ignition timing criteria, differs by only $\Delta CA50 = 1.9^{\circ}$ for these two cycles making it difficult to detect the misfire cycle.

Cyclic Variation of Ignition Timing

For all 329 operating points, 100 engine cycles are collected and the combustion metrics of P_{max}, θ_{Pmax} and $CA50$ are calculated for each of the 100 cycles. A measure of the cyclic variation of P_{max}, θ_{Pmax} and $CA50$ are determined by taking the standard deviation of the 100 cycle values of each and are denoted σ_{Pmax}, $\sigma_{\theta_{Pmax}}$ and σ_{CA50} respectively and used to represent combustion cyclic variability at each operating point. Cyclic variations of P_{max} (σ_{Pmax}) as a function of $\sigma_{\theta_{Pmax}}$ and σ_{CA50} for each of the 329 operating points are shown in Figure 5. In this plot, σ_{Pmax} appears linearly correlated with $\sigma_{\theta_{Pmax}}$ indicating that the variation in the location of the maximum crank angle pressure $\sigma_{\theta_{Pmax}}$ is correlated to the variation of the maximum pressure σ_{Pmax}. However, for cases with high cyclic variations ($\sigma_{CA50} > 2CAD$), this correlation is not apparent between $\sigma_{P_{max}}$ and σ_{CA50}.

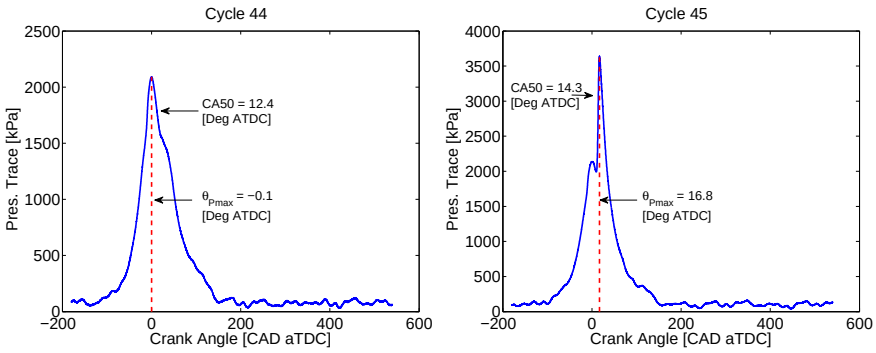

Figure 4: Cylinder pressure trace of two consecutive cycles for HCCI combustion at point A. Misfire (left) and normal combustion (right) (conditions as Figure 3)

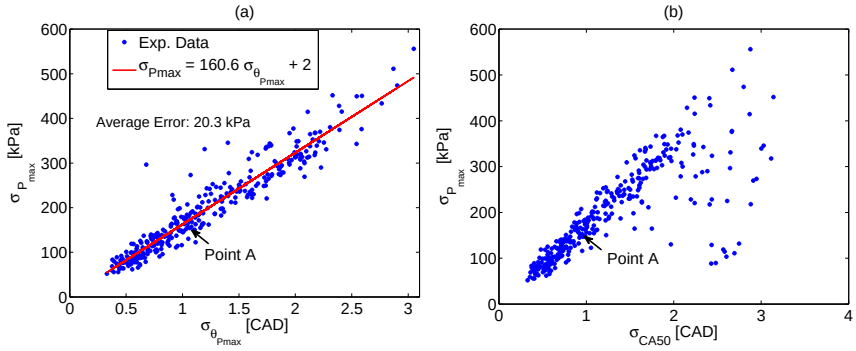

Figure 5: Cyclic variations of P_{max} versus θ_{Pmax}

The 100 cycle mean of the combustion metrics θ_{Pmax} and $CA50$ for each of the 329 operating points is calculated and plotted in Figure 6(a). θ_{Pmax} correlates linearly with $CA50$ with an average error of 0.3, as shown in Figure 6(a). The cyclic variations of $\sigma_{\theta_{Pmax}}$ correlate with σ_{CA50} only when cyclic variations of $CA50$ are low ($STD_{CA50} \leq 2CAD$), as shown in Figure 6(b). For the cases with high cyclic variations ($STD_{CA50} > 2CAD$), different ranges of cyclic variations for $\sigma_{\theta_{Pmax}}$ are visible. This corresponds to different combustion modes of normal and misfire while having a fixed same standard deviation for $CA50$. Thus $CA50$ does not serve as a proper indicator for distinguishing different regimes of combustion in those cases.

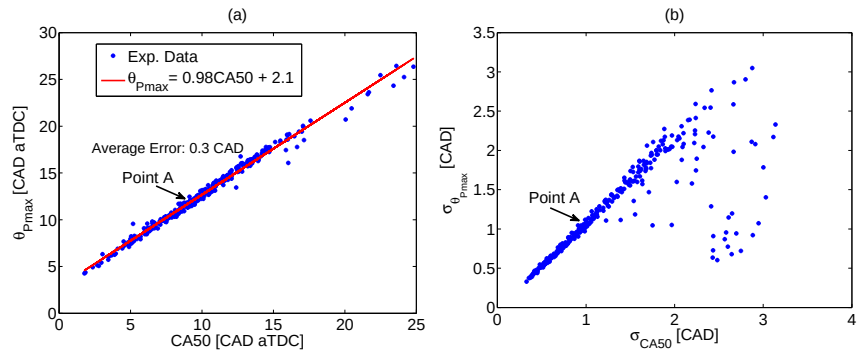

Figure 6: θ_{Pmax} versus location of CA50 and STD of θ_{Pmax} versus STD of CA50

IMEP values for changing θ_{Pmax} are plotted in Figure 7 for two different scenarios: (a) constant fueling rate (variable ϕ) and (b) variable fueling rate (constant ϕ). In Figure 7(a), combustion timing (θ_{Pmax}) advances from 17 to 6 [Deg ATDC] by increasing the intake pressure from 96 to 138 kPa at a constant fueling rate. Increasing the intake pressure results in a large air change in the cylinder, which due to constant injected fuel, causes a leaner mixture (ϕ of 0.61 $\longrightarrow$ 0.38). IMEP increases in Figure 7(a) as the combustion timing advances towards TDC. By varying combustion timing in Figure 7(a) IMEP changes about 0.5 bar or 10% change in the engine thermal efficiency at this base condition of 5 bar IMEP. This clearly shows that combustion timing directly influences engine performance. In Figure 7(b), an opposite

trend compared with Figure 7(a) is shown. Here IMEP decreases when advancing the combustion timing to TDC. In Figure 7(b) as θ_{Pmax} advances slightly from 6.45 to 6.1 [Deg ATDC] by increasing the intake temperature from 73 to 112 °C and keeping (ϕ) constant by increasing the fueling rate from 0.357 kg/h to 0.379 kg/h. IMEP in Figure 7(b) follows the same trend as that of the fuel mass flowrate and increases when the fuel rate is increased. A comparison between Figure 7(a) and (b) indicates that IMEP is more strongly influenced by fueling rate rather than the ignition timing, but depends on the ignition timing for the conditions that have a constant fueling rate.

A linear normalized sensitivity function ($S_x = \frac{\partial \theta_{Pmax}}{\partial X} \times \frac{X}{\theta_{Pmax}} \times 100$) is used to analyze the sensitivity of θ_{Pmax} to the variations to each of two different parameters (X). The two parameters are: ϕ and $\dot{m}_{fuel}$. Sensitivity analysis is done around two operating points with conditions outlined in Table 3.

Table 3: Base conditions used for the sensitivity analysis

	PRF	N [rpm]	T_{man} [°C]	P_{man} [kPa]	ϕ	$\dot{m}_{fuel}$ [kg/h]	EGR %	$T_{coolant}$ [°C]	T_{oil} [°C]
Figure 7(a)	40	810	75	96.2	0.606	0.31	0	73	75
Figure 7(b)	10	1000	81	119.7	0.42	0.36-0.38	0	74	63

The sensitivity of θ_{Pmax} to ϕ at constant fueling (Figure 7(a)) is $S_\phi = 144\%$ while the sensitivity of θ_{Pmax} to $\dot{m}_{fuel}$ at constant ϕ (Figure 7(b)) is $S_{\dot{m}_{fuel}} = 828\%$. The sensitivity of HCCI combustion timing helps to understand how to control HCCI timing effectively. For the controller of HCCI combustion timing, it is essential to know which of the charge variables are more significant than the others and which charge variable is more dominant in a competition to affect the combustion timing.

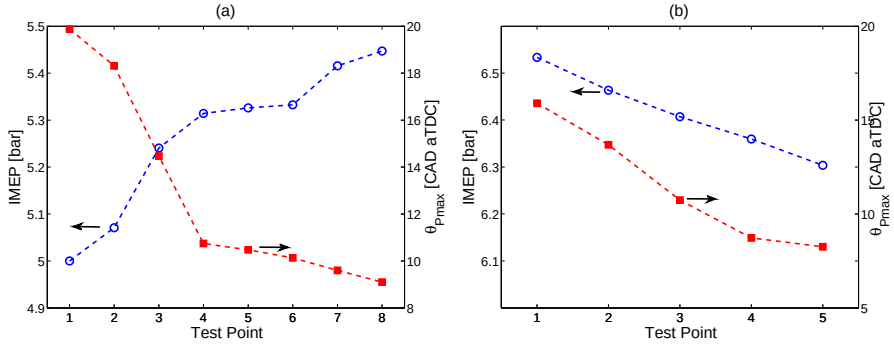

Figure 7: IMEP versus θ_{Pmax} for (a) constant fueling rate (0.31 $\pm$ 0.003 kg/h), PRF40, N = 810r/min, EGR = 0 %, T_m = 75 °C; (b) variable fueling rate and intake temperature, PRF10, $\phi = 0.42$, N = 1000r/min, EGR = 0 %, P_m = 119.8 $\pm$ 0.2 kPa

6. Summary

Experimental data from HCCI engine collected at 329 operating points is used to evaluate the performance of a new ignition timing criteria θ_{Pmax} over a wide range of operating conditions. θ_{Pmax} is better able to distinguish between the normal and misfire combustion cycles than $CA50$, particularly near partial burn region. Correlations between θ_{Pmax} and P_{max}, $CA50$ and $IMEP$ are investigated at different conditions in order to confirm the validity of this new ignition timing criteria. θ_{Pmax} is found to be a good ignition timing criteria to distinguish between normal and misfire operation. $CA50$ is found to be a poor measure of cyclic variations for this engine when the standard deviation of $CA50$ of an operating point is greater than 2 crank angle degrees.

Acknowledgments AUTO21 Network of Centres of Excellence, the Canadian Foundation for Innovation (CFI) and the Natural Sciences and Engineering Research Council of Canada (NSERC) are gratefully acknowledged.

References

[1] X. Lu and W. Chen and Y. Hou and Z. Huang . Study on Ignition, Combustion and Emissions of HCCI Combustion Engines Fueled with Primary Reference Fuels . *SAE Paper No. 2005-01-0155.*, 2005.

[2] M. Yao, Z. Zheng, B. Zhang, and Z. Chen. The Effect of PRF Fuel Octane Number on HCCI Operation. *SAE Paper No. 2004-01-2992*, 2004.

[3] F. Ponti. Developmnet of a Torsional Behavior Powertrain Model for Multiple Misfire Detection. *Journal of Engineering for Gas Turbines and Power*, 130:022803 1–13, 2008.

[4] Z. Wu and A. Lee. Misfire Detection Using a Dynamic Neural Network with Output Feedback. *SAE Paper No. 980515*, 1998.

[5] D. Moro, P. Azzoni, and G. Minelly. Misfire Pattern Recognition in High-Performance SI 12-cylinder Engine. *SAE Paper No. 980521*, 1998.

[6] H. Zhao. *HCCI and CAI engines for the automotive industry*. Woodhead Publishing Limited, 2007.

[7] J.B. Heywood. *Internal Combustion Engine Fundamentals*. McGraw HILL, 1988.

[8] A. Ghazimirsaied, M. Shahbakhti, and C.R. Koch. HCCI Engine Combustion Phasing Prediction Using a Symbolic-Statistics Approach. *Journal of Engineering for Gas Turbines and Power*, 132:082805 1–5, 2010.

[9] M. Shahbakhti, A. Ghazimirsaied, and C.R. Koch. Experimental Study of the Variation in a Exhaust Temperature in a HCCI Engine . *Proc. IMechE Part D: Journal of Automobile Engineering*, 224:1177–1197, 2010.

[10] M. Shahbakhti and C.R. Koch. Characterizing the Cyclic variability of ignition timing in a homogenous charge compression ignition engine fueled with n-heptane/iso-octane blend fuels. *International Journal of Engine Research*, 9:361 – 397, 2008.

[11] K. L. Knierim, S. Park, J. Ahmed, and A. Kojic. Simulation of Misfire and Strategies for Misfire Recovery of Gasoline HCCI. *American Control Conference, Palo Alto, USA*, June 2008.

[12] I. Haskara and L. Mianzo. Real-time and Indicated Torque Estimation via Second Order Sliding Modes . *Proceedings of the American Control Conference, Arlington, USA*, June 2001.

[13] E.A. VanDyne and C.L. Burckmyer and A.M. Wahl and A.E. Funaioli. Misfire Detection From Ionization Feedback Utilizing the Smartfire Plasma Ignition Technology. *SAE Paper No. 2000-01-1377.*, 2000.

[14] F.L. Bue, A.D. Stefano, C. Giaconia, and E. Pipitone. Misfire Detection System based on the Measure of Crankshaft Angular Velocity. *Proceeding of the 11th annual AMAA conference, Berlin*, March 2007.

[15] R. Lupul. Steady State and Transient Characterization of a HCCI Engine with Varying Octane Fuel. Master's thesis, University of Alberta, 2008.

[16] A.D. Audet. Closed Loop Control of HCCI using Camshaft Phasing and Dual Fuels. Master's thesis, University of Alberta, 2008.

[17] U. Asad and M. Zheng. Fast Heat Release Characterization of a Diesel Engine. *J Thermal Sci.*, 47:1688–1700, 2008.

[18] F.A. Matekunas. Modes and Measures of Cyclic Combustion Variability. *SAE Paper No. 830337*, 1983.

[19] A. Ghazimirsaied, M. Shahbakhti, and C.R. Koch. Comparison of Crankangle Based Ignititon Timing Methods on an HCCI Engine. *Submitted to the Proceeding of the ASME Internal Combustion Engine Division 2010 Fall Conference, San Antonio, USA.*, 2010.